Phytochemistry 71 (2010) 168–178

Contents lists available at ScienceDirect

Phytochemistry

journal homepage: www.elsevier.com/locate/phytochem

Over-expression of *Arabidopsis thaliana* carotenoid hydroxylases individually and in combination with a β-carotene ketolase provides insight into *in vivo* functions

Ji-Eun Kim [a], Kimberly M. Cheng [a], Neal E. Craft [b], Björn Hamberger [c], Carl J. Douglas [c,*]

[a] Department of Animal Science, University of British Columbia, Vancouver, BC, Canada V6T1Z4
[b] Craft Technologies, Inc., Wilson, NC 27892, USA
[c] Department of Botany, University of British Columbia, Vancouver, BC, Canada V6T1Z4

ARTICLE INFO

Article history:
Received 14 September 2008
Received in revised form 11 February 2009
Available online 24 November 2009

Keywords:
Arabidopsis thaliana
Cruciferae
Thale CMSS
Ketocarotenoid
*P*450 hydroxylase
Ketolase
β-Carotene hydroxylase
bkt1
CrtO
Cytochrome *P*450

ABSTRACT

Carotenoids represent a group of widely distributed pigments derived from the general isoprenoid biosynthetic pathway that possess diverse functions in plant primary and secondary metabolism. Modification of α- and β-carotene backbones depends in part on ring hydroxylation. Two ferredoxin-dependent non-heme di-iron monooxygenases (AtB1 and AtB2) that mainly catalyze *in vivo* β-carotene hydroxylations of β,β-carotenoids, and two heme-containing cytochrome *P*450 (CYP) monooxygenases (CYP97A3 and CYP97C1) that preferentially hydroxylate the ε-ring of α-carotene or the β-ring of β,ε-carotenoids, have been characterized in *Arabidopsis* by analysis of loss-of-function mutant phenotypes. We further investigated functional roles of both hydroxylase classes in modification of the β- and ε-rings of α-carotene and β-carotene through over-expression of *AtB1*, *CYP97A3*, *CYP97C1*, and the hydroxylase candidate *CYP97B3*. Since carotenoid hydroxylation is required for generation of ketocarotenoids by the *bkt1*(*CrtO*) β-carotene ketolase, all hydroxylase constructs were also introduced into an *Arabidopsis* line expressing the *Haematococcus pluvalis bkt1* β-carotene ketolase. Analysis of foliar carotenoid profiles in lines over-expressing the individual hydroxylases indicate a role for CYP97B3 in carotenoid biosynthesis, confirm and extend previous findings of hydroxylase activities based on knock-out mutants, and suggest functions of the multifunctional enzymes in carotenoid biosynthesis. Hydroxylase over-expression in combination with *bkt1* did not result in ketocarotenoid accumulation, but instead unexpected patterns of α-carotene derivatives, accompanied by a reduction of α-carotene, were observed. These data suggest possible interactions between the β-carotene ketolase bkt1 and the hydroxylases that impact partitioning of carbon flux into different carotenoid branch pathways.

1. Introduction

Xanthophylls are oxygenated derivatives of carotenes that perform critical roles in the photosynthetic apparatus of higher plants (Niyogi, 1999). Lutein (3*R*,3′*R*-β,ε-carotene-3,3′-diol) (**8**) is the most abundant xanthophyll in plant photosynthetic tissues, where it plays an important role in light harvesting complexes (Tian et al., 2004) (Fig. 1). Zeaxanthin (3*R*,3′*R*-β,β-carotene-3,3′-diol) (**7**) is a structural isomer of lutein (**8**) and a component of the non-photochemical quenching mechanism (Cunningham and Gantt, 1998). Both lutein (**8**) and zeaxanthin (**7**) are dihydroxylated xanthophylls. Lutein (**8**) is generated by addition of hydroxyl groups to the 3,3′ positions of the ε- and β-rings of α-carotene (**5a**) (β,ε-ring carotene) via action of ε- and β-ring hydroxylases. Zeaxanthin (**9**) is formed by addition of hydroxyl groups to the 3,3′ position of both β-rings of β-carotene (**5b**) (β,β-ring carotene) via β-hydroxylases. (DellaPenna, 2004) (Fig. 1).

In addition to the *Arabidopsis thaliana AtB1* and *AtB2* non-heme carotenoid hydroxylases (Sun et al., 1996; Tian and DellaPenna, 2004), non-heme β-carotene β-ring hydroxylases from photosynthetic and nonphotosynthetic bacteria, green algae and other plants have been cloned and functionally characterized by heterologous expression (Misawa et al., 1990; Hundle et al., 1994; Misawa et al., 1995; Bouvier et al., 1998; Cunningham and Gantt, 1998; Masamoto et al., 1998; Linden, 1999; Galpaz et al., 2006). In plants, heme-containing cytochrome *P*450 (CYP) monooxygenases play important roles in biosynthesis of secondary metabolites, often as hydroxylases, but most are of unknown biochemical function. Two cytochrome *P*450-type monooxygenases with activity against carotenoids have been identified from phenotypes of knock-out mutants of *Arabidopsis*. CYP97C1, encoded by the *LUT1* locus has α-carotene (**5a**) ε-ring hydroxylase activity (Tian et al., 2004), and CYP97A3 (*LUT5* locus) encodes a β-ring hydroxylase (**5b**) with major activity towards the β-ring of α-carotene (**5a**) and minor

* Corresponding author. Tel.: +1 604 822 2618; fax: +1 604 822 6089.
E-mail address: cdouglas@interchange.ubc.ca (C.J. Douglas).

0031-9422/$ - see front matter © 2009 Elsevier Ltd. All rights reserved.
doi:10.1016/j.phytochem.2009.10.011

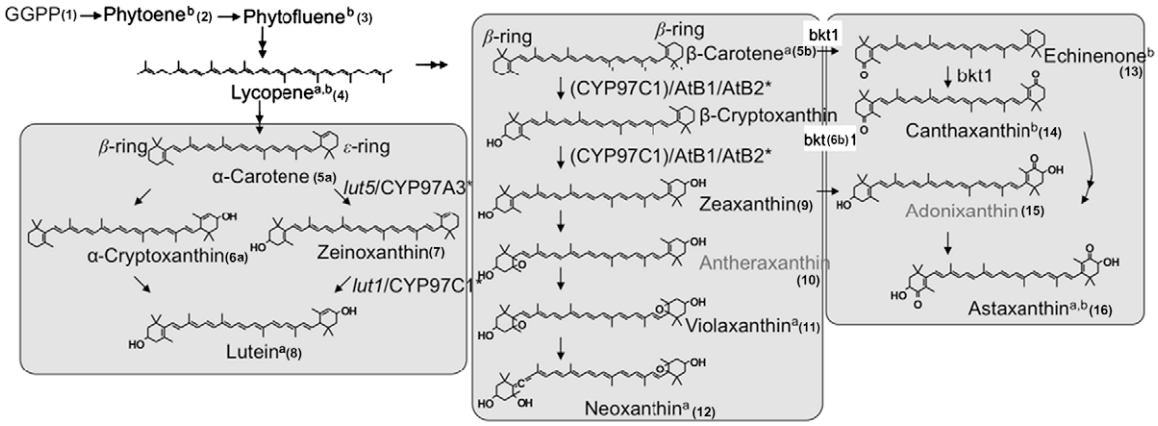

Fig. 1. Schematic carotenoid biosynthesis pathways: the α- and β-carotenoid routes to the major metabolites lutein and neoxanthin and the non-plant astaxanthin pathway. Compounds shown in black were assayed in this study, identified and quantified using authentic standards where applicable. Key hydroxylation enzymes (AtB, CYP97A3, CYP97B3, CYP97C1), overexpressed in this study are indicated at the pathway step deduced from mutant phenotype analysis or heterologously expressed enzymes. *Tian et al. (2004), Fiore et al. (2006), and Kim and DellaPenna (2006). [a]Compounds assayed for both *cis*- and *trans* isoforms. [b]Concentration of compound below detection limit in all samples.

activity on the β-ring of β-carotene (**5b**) (Kim and DellaPenna, 2006).

Recently, two cytochrome *P*450-type carotenoid hydroxylases (CYP97A4 and CYP97C2) have been isolated from *Oryza sativa* (rice) and characterized in a β-carotene producing *Escherichia coli* strain (Quinlan et al., 2007). Rice CYP97A4 and CYP97C2, which group in the same clan as CYP97A3 and CYP97C1, have ε-ring hydroxylase and β-ring hydroxylase activities, respectively. Furthermore, CYP175A1, cloned from the thermostable bacterium *Thermus thermophilus* HB27, shows β-ring hydroxylase activity in *E. coli*, hydroxylating both β-rings of β-carotene (**5b**) to form zeaxanthin (**9**) (Blasco et al., 2004). Therefore, there is clear evidence that *P*450-type monooxygenases, in addition to non-heme hydroxylases such as AtB1, are involved in carotenoid hydroxylation pathways.

Genetic studies suggest that there may be additional uncharacterized carotenoid hydroxylase(s) involved in the biosynthesis of the β-,β-ring xanthophylls or β-,ε-ring xanthophylls, since residual accumulation of hydroxylated carotenoids was observed in mutants lacking activity of the known hydroxylases (Tian et al., 2004; Fiore et al., 2006; Kim and DellaPenna, 2006). CYP97B3, an uncharacterized *P*450 monoxygenase that shares 42% amino acid identity with CYP97C1 and is phylogenetically closely related (Tian et al., 2004), was hypothesized to have β-carotene hydroxylase activity (Kim et al., 2005). In that study, a potential role for CYP97B3 in hydroxylation of β-carotene (**5b**) was demonstrated by expressing the recombinant enzyme in a β-carotene producing *E. coli* strain. This analysis provided evidence that CYP97B3 could hydroxylate the β-rings of β-carotene (**5b**), generating β-cryptoxanthin (**6b**) and zeaxanthin (**9**).

Ketocarotenoids, a family of xanthophyll ketone derivatives of β-carotene (**5b**) with strong antioxidant activity, have gained attention due to their antioxidant properties and potential health promoting benefits as nutraceuticals (Martín et al., 2008), and their use as additives in feed for pigmentation of fish and crustaceans (Gerjets et al., 2007). However, these compounds are not widely found in plants. Genes encoding β-carotene ketolase (β-C-4-oxygenase) were originally cloned from green algae and bacteria (Britton, 1998). The algal *Haematococcus pluvialis* bkt1 ketolase (Huang et al., 2005; previously referred to as CrtO) generates ketone derivatives of hydroxylated β-carotene derivatives to produce astaxanthin (**16**) (3,3′-dihydroxy-4,4′-diketo-β,β-carotene), and three *bkt* genes have been identified from *H. pluvialis* (Huang et al., 2005) (Fig. 1). In plants, ketocarotenoids are found in some angiosperm taxa, for example in *Adonis* spp. where they accumulate at levels of up to 1% of dry weight in flowers (Renstrom et al., 1981). A ketolase gene (*AdoKETO*) was cloned from *Adonis aestivalis* and the enzyme characterized in both *E. coli* and *Arabidopsis* (Cunningham and Gantt, 2005; Yu et al., 2006). Like the *Arabidopsis* β-ring AtB1 hydroxylase, the *A. aestivalis* and *H. pluvialis* ketolases are members of a large class of membrane-intergral, di-iron oxygenase enzymes (Cunningham and Gantt, 1998, 2005).

In this study, we have further investigated the hypothesis that in addition to CYP97A3 and CYP97C1, CYP97B3 plays a role in the hydroxylation of the β-ring of α-carotene (**5a**) and β-carotene (**5b**) in plants. To test this hypothesis, we generated *Arabidopsis* lines overexpressing *AtB1*, *CYP97A3*, *CYP97B3*, and *CYP97C1* by placing them under the control of a double CaMV35S promoter, and determined the metabolic consequences of over-expression with respect to carotenoid accumulation in leaf tissue. With the additional goal of exploring alternative ways of engineering the production of novel ketocarotenoids in higher plants, we also generated a double *CaMV35S-bkt1* ketolase construct using a *H. pluvialis bkt1* gene. We used a co-transformation approach to generate transgenic *Arabidopsis* lines expressing the *bkt1* ketolase alone and lines expressing both the *bkt1* ketolase and each of the four candidate carotenoid hydroxylases. We then profiled carotenoid accumulation in leaves of these lines relative to untransformed control plants. Our data provide new insights on the roles of *P*450 hydroxylases in α-carotene (**5a**) and β-carotene (**5b**) modification, and we present evidence for metabolic cross-talk between carotenoid metabolic pathways.

2. Results

2.1. Selection of single and co-transformed plants

We transformed *Arabidopsis* Col-0 plants with single *Agrobacterium* strains harboring *AtB1*, *CYP97A3*, *CYP97B3*, or *CYP97C1* under the control of a double CaMV 35S promoter, or two separate *Agrobacterium* strains harboring one of these constructs and the *bkt1* gene under control of a double CaMV35S promoter, as described in Section 5. T2 seedlings of self-pollinated co-transformed T1 lines were selected sequentially for hygromycin and BASTA resistance specific to the T-DNAs of the two strains to identify co-transformed progeny. We obtained between 10 and 31 transgenic lines containing each of the following single transgenes (line designation in

brackets): 2×35S::AtB1 (AtB1), 2×35S::CYP97A3 (97A3), 2×35S::CYP97B3 (97B3), 2×35S::CYP97C1 (97C1) and 2×35S::KB (*bkt1* ketolase; KB). In addition, we obtained between 8 and 10 co-transformed lines harboring both *AtB1* or one of the three *P*450 genes in combination with *bkt1*, designated as follows: AtBKB, 97AKB, 97BKB and 97CKB. The presence of the transgene(s) was verified by PCR analysis of genomic DNA isolated from T1 plants. No morphological differences in the transgenic lines relative to wild-type plants were observed.

2.2. Transcript levels in single and co-transformed plants

Reverse transcription-PCR (RT-PCR) was performed using RNA isolated from rosette leaves of each T2 line to evaluate the transcript level of each transgene relative to wild-type plants. Figs. 2 and 3 show representative examples of these analyses with all individual lines used for analysis indicated. Transcript levels for *AtB1*, *CYP97A3*, *CYP97B3*, and *CYP97C1* were very low, but detectable, by RT-PCR in wild-type plants, suggesting low levels of endogenous gene expression (Figs. 2 and 3). As expected, no ketolase expression was detected in wild-type plants (Fig. 2E). Among the multiple lines generated, we identified two representative over-expression lines with high *AtB1*, *CYP97A3*, *CYP97B3*, and *CYP97C1* and *bkt1* expression levels. Fig. 2 shows examples of single transformant lines with high transgene expression (AtB1-1 and AtB1-3, 97A3-1 and 97A3-2, 97B3-1 and 97B3-3, 97C1-2 and 97C1-3, KB-2 and KB-3), and Fig. 3 shows examples of double transformed lines with high levels of expression of both transgenes (individual hydroxylases combined with *bkt1* ketolase; AtBKB-2 and AtBKB-3, 97AKB-1 and 97AKB-2, 97BKB-1 and 97BKB-2, and 97CKB-1).

Two independent and representative lines with the highest expression levels for each single and double gene combination, shown in bold in Figs. 2 and 3, were chosen for carotenoid metabolite profiling by HPLC.

2.3. Carotenoid profiling

We generated T3 homozygous lines for most of the T2 lines overexpressing single or double transgene combinations that were chosen for further analysis, and rosette leaves from two individual T3 plants of each line were harvested for HPLC analysis of carotenoid content. Following carotenoid extraction, each sample was analyzed twice and the mean of the two runs was used for statistical analysis. We were unable to obtain T3 homozygous plants for one of the 97BKB lines high expressing lines, so one 97BKB line heterozygous for both transgenes (with high expression for both genes) was used.

The presence of 21 carotenoids (including isomers) was assayed by co-chromatography with authentic standards and concentrations of the following were determined as detailed in Section 5: *trans*-lycopene (**4b**), *cis*-lycopene (**4a**), phytoene (**2**), phytofluene (**3**), echinenone (**13**), canthaxanthin (**14**), *trans*-astaxanthin (**16**), *cis*-astaxanthin (**16**), α-carotene (**5a**), α-cryptoxanthin (**6a**), zeinoxanthin (**7**), *trans*-lutein (**8**), *cis*-lutein (**8**), *trans*-β-carotene (**5b**), *cis*-β-carotene (**5b**), β-cryptoxanthin (**6b**), *trans*-zeaxanthin (**9**), *trans*-violaxanthin (**11**), *cis*-violaxanthin (**11**), *trans*-neoxanthin (**12**), and *cis*-neoxanthin (**12**), Of these, concentrations of echinenone (**13**), canthaxanthin (**14**), *trans*-astaxanthin (**16**), *cis*-astaxanthin (**16**), *trans*-lycopene (**4**), *cis*-lycopene (**4**), phytoene (**2**), and phytofluene (**3**) were below detectable levels in all samples.

Tables 1 and 2 summarize the carotenoid concentrations measured in wild-type and the single or double transformation lines.

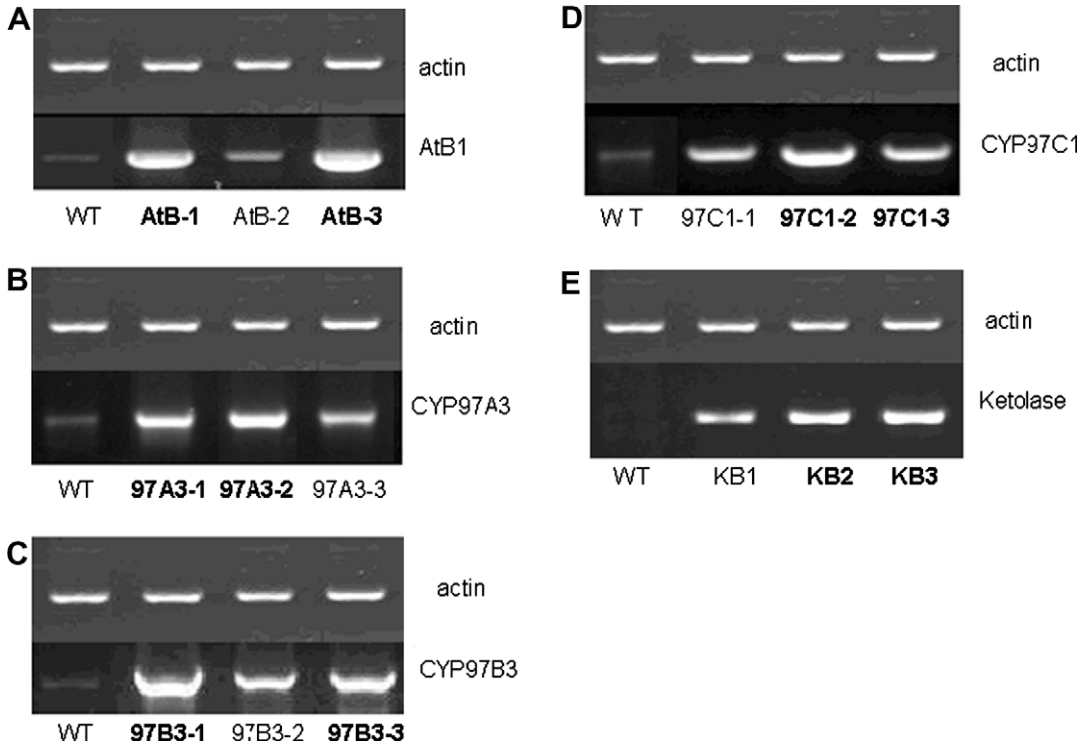

Fig. 2. Transgene expression levels in individual lines harboring single hydroxylase or ketolase transgenes. RT-PCR was carried out on RNA isolated from T2 lines, and from a wild-type control line. PCR cycle numbers were adjusted so that amplification actin transcripts were was not saturated. An actin control was included for each cDNA sample, to normalize for variations in cDNA amount. Expression in representative lines for each construct is shown. (A) **AtB1** single transgenic lines; (B) **CYP97A3** single transgene lines; (C) **CYP97B3** single transgene lines; (D) **CYP97C1** single transgenic lines; (E) **ketolase** single transgenic lines. **WT**, wild-type control line. **Lines 1–3**, individual T2 lines for each transgene. High expression lines (bold fonts) were used to HPLC analysis.

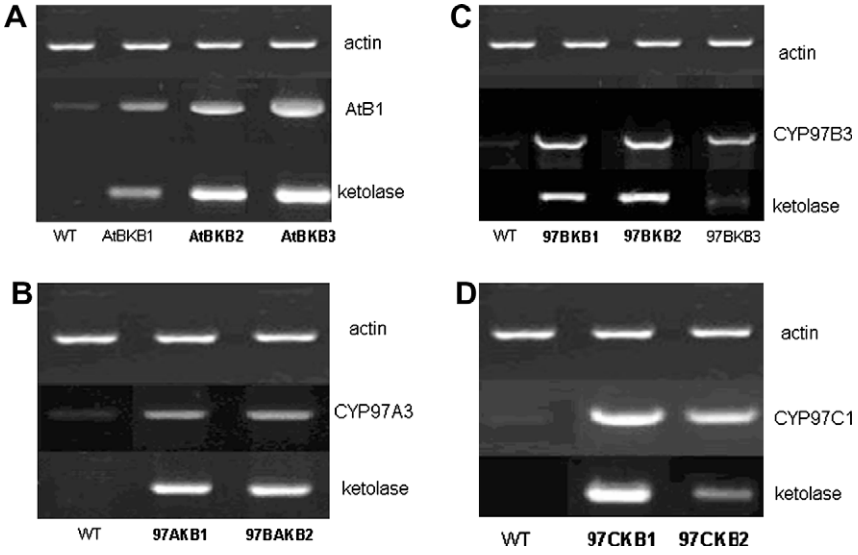

Fig. 3. Transgene expression levels in lines harboring both hydroxylase and ketolase trangenes. RT-PCR was carried out on RNA isolated from T2 lines, and from a wild-type control line. PCR cycle numbers were adjusted so that amplification actin transcripts were was not saturated. An actin control was included for each cDNA sample, to normalize for variations in cDNA amount. Expression in representative lines for each construct and double transformants are shown. (A) **AtBKB**: AtB1 and ketolase double transgene lines, (B) **97AKB**: CYP97A3 and ketolase double transgene lines, (C) **97BKB**: CYP97B3 and ketolase transgene lines, (D) **97CKB**: CYP97C1 and ketolase transgene lines. **WT**, wild-type control line. **Lines 1–3**, individual T2 lines for each double transgene. High expression lines (bold fonts) were used to HPLC analysis.

Table 1
Profiling of carotenoids derived from α-carotene (**5a**) in *Arabidopsis* wild-type plants and over-expression lines.

Line	Carotenoid amount (μg g^{-1} of leaf tissue)				
	α-Carotene (**5a**)	α-Cryptoxanthin (**6a**)	Zeinoxanthin (**7**)	*trans*-Lutein (**8**)	*cis*-Lutein (**8**)
WT	1.27 ± 0.12^{a}	0.27 ± 0.04^{a}	0.24 ± 0.04^{d}	88.8 ± 7.28^{a}	6.33 ± 1.03^{bc}
AtB1	1.06 ± 0.08^{ab}	0.13 ± 0.03^{cd}	0.29 ± 0.03^{cd}	69.0 ± 5.15^{a}	8.19 ± 0.73^{ab}
AtBKB	0.84 ± 0.08^{bc}	0.19 ± 0.03^{abc}	0.34 ± 0.03^{abc}	75.4 ± 5.15^{a}	6.63 ± 0.73^{bc}
97A3	0.84 ± 0.08^{bc}	0.23 ± 0.03^{ab}	0.30 ± 0.03^{bcd}	80.6 ± 5.15^{a}	8.04 ± 0.73^{ab}
97AKB	0.75 ± 0.08^{c}	0.15 ± 0.03^{bcd}	0.37 ± 0.03^{abc}	75.2 ± 5.15^{a}	8.72 ± 0.73^{ab}
97B3	0.79 ± 0.08^{c}	0.16 ± 0.03^{bcd}	0.40 ± 0.03^{a}	73.5 ± 5.15^{a}	7.15 ± 0.73^{ab}
97BKB	0.80 ± 0.08^{c}	0.16 ± 0.03^{bcd}	0.37 ± 0.03^{ab}	80.6 ± 5.15^{a}	9.26 ± 0.73^{a}
97C1	0.79 ± 0.08^{c}	0.20 ± 0.03^{abc}	0.34 ± 0.03^{abc}	91.2 ± 5.15^{a}	6.62 ± 0.73^{bc}
97CKB	0.60 ± 0.12^{c}	0.08 ± 0.03^{d}	0.39 ± 0.04^{ab}	88.0 ± 7.28^{a}	8.60 ± 1.03^{ab}
KB	0.72 ± 0.08^{c}	0.19 ± 0.04^{abc}	0.23 ± 0.03^{d}	75.2 ± 5.15^{a}	4.97 ± 0.73^{c}

Carotenoid amounts were determined using method (2) as detailed in Section 5. Least-Squares means followed by the same letters are not significantly different ($P > 0.05$) by Least-Squares Analysis of Variance. In addition, values highlighted in grey are significantly different between transgenic lines in wild type. Since each SE was internally adjusted in the Least-Squares Analysis, treatment with the same sample size will have the same SE value. Lines are abbreviated as follows: **WT**, wild-type; **AtB1**, 2×35S::AtB1; **AtBKB**, 2×35S::AtB1 and 2×35S::*bkt1*; **97A3**, 2×35S::97A3; **97AKB**, 2×35S::97A3 and 2×35S::*bkt1*; **97B3**, 2×35S::97B3; **97BKB**, 2×35S::97B3 and 2×35S::*bkt1*; **97C1**, 2×35S::97C1; **97CKB**, 2×35S::97C1 and 2×35S::*bkt1*; **KB**, 2×35S::*bkt1*.

Table 2
Profiling of carotenoids derived from β-carotene (**5b**) in *Arabidopsis* wild-type plants and over-expression lines.

Line	Carotenoid amount (μg g^{-1} of leaf tissue)						
	β-Carotene (**5b**)	β-Cryptoxanthin (**6b**)	Zeaxanthin (**9**)	*trans*-Violaxanthin (**11**)	*cis*-Violaxanthin (**11**)	*trans*-Neoxanthin (**12**)	*cis*-Neoxanthin (**12**)
WT	41.8 ± 2.70^{a}	0.39 ± 0.04^{b}	0.79 ± 0.23^{bcd}	14.7 ± 1.17^{b}	2.60 ± 0.23^{cd}	14.3 ± 7.28^{b}	12.0 ± 1.03^{a}
AtB1	38.2 ± 1.91^{a}	0.51 ± 0.02^{a}	1.58 ± 0.16^{a}	31.0 ± 0.83^{a}	6.45 ± 0.16^{a}	30.6 ± 5.15^{a}	6.6 ± 0.73^{a}
AtBKB	38.1 ± 1.91^{a}	0.32 ± 0.02^{bcd}	0.54 ± 0.16^{d}	14.5 ± 0.83^{b}	2.76 ± 0.16^{bcd}	14.2 ± 5.15^{b}	8.9 ± 0.73^{a}
97A3	41.7 ± 1.91^{a}	0.36 ± 0.02^{bc}	1.62 ± 0.16^{a}	15.0 ± 0.83^{b}	3.00 ± 0.16^{bc}	14.6 ± 5.15^{b}	9.2 ± 0.73^{a}
97AKB	36.9 ± 1.91^{a}	0.30 ± 0.02^{bcd}	1.55 ± 0.16^{a}	13.2 ± 0.83^{b}	2.82 ± 0.16^{bcd}	12.8 ± 5.15^{b}	6.7 ± 0.73^{a}
97B3	36.7 ± 1.91^{a}	0.22 ± 0.02^{e}	1.33 ± 0.16^{ab}	14.6 ± 0.83^{b}	2.83 ± 0.16^{bcd}	4.0 ± 5.15^{b}	8.8 ± 0.73^{a}
97BKB	44.5 ± 1.91^{a}	0.29 ± 0.02^{bcde}	0.66 ± 0.16^{cd}	14.7 ± 0.83^{b}	3.21 ± 0.16^{b}	14.3 ± 5.15^{b}	7.5 ± 0.73^{a}
97C1	41.3 ± 1.91^{a}	0.28 ± 0.02^{de}	1.47 ± 0.16^{abc}	14.1 ± 0.83^{b}	2.73 ± 0.16^{bcd}	13.6 ± 5.15^{b}	11.3 ± 0.73^{a}
97CKB	37.6 ± 2.70^{a}	0.28 ± 0.04^{bcde}	1.19 ± 0.23^{abc}	13.8 ± 1.17^{b}	2.60 ± 0.23^{cd}	13.6 ± 7.28^{b}	7.6 ± 1.03^{a}
KB	39.8 ± 1.91^{a}	0.34 ± 0.02^{bcd}	0.77 ± 0.16^{cd}	13.8 ± 0.83^{b}	2.46 ± 0.16^{d}	13.4 ± 5.15^{b}	10.1 ± 0.73^{a}

Carotenoid amounts were determined using method (2) as detailed in Section 5. Least-Squares means followed by the same letters are not significantly different ($P > 0.05$) by Least-Squares Analysis of Variance. In addition, values highlighted in grey are significantly different between transgenic lines in wild type. Since each SE was internally adjusted in the Least-Squares Analysis, treatment with the same sample size will have the same SE value. Lines are abbreviated as follows: **WT**, wild-type; **AtB1**, 2×35S::AtB1; **AtBKB**, 2×35S::AtB1 and 2×35S::*bkt1*; **97A3**, 2×35S::97A3; **97AKB**, 2×35S::97A3 and 2×35S::*bkt1*; **97B3**, 2×35S::97B3; **97BKB**, 2×35S::97B3 and 2×35S::*bkt1*; **97C1**, 2×35S::97C1; **97CKB**, 2×35S::97C1 and 2×35S::*bkt1*; **KB**, 2×35S::*bkt1*.

Results are presented as the means of two independently generated transgenic lines for each construct or construct combination, with two independent samples extracted and analyzed from each independent transgenic line. Every sample was injected twice. A summary of the results for the different lines follows.

WT: HPLC analysis of wild-type Col-0 plants showed that lutein (**8**) and β-carotene (**5b**) were the major products in leaves (Tables 1 and 2). As expected, no ketocarotenoids (astaxanthin (**16**), canthaxanthin (**14**), echienone (**13**)) were detected.

AtB1 and AtBKB: compared with WT, over-expression of *AtB1* resulted in significant increases in products derived from β-carotene (**5b**) (Table 2), but had little effect on products derived from α-carotene (**5a**) (Table 1). AtB1 lines had significantly ($p < 0.05$) higher concentrations of all β-carotene (**5b**) derived compounds assayed except cis-neoxanthin (**12**) (highlighted AtB1 values, Table 2). Among α-carotene (**5a**) derivatives, AtB1 plants had a significantly lower concentration only of α-cryptoxanthin (**6a**). These data suggest that over-expression of AtB1 results in a significant shift of metabolic flux into the production of β-carotene derivatives.

In the *AtB1*/*bkt1* co-transformed lines (AtBKB) no ketocarotenoid products were detected despite high expression of the *bkt1* ketolase (Fig. 3A). Furthermore, the increased levels of all β-carotene derivatives seen in AtB1 lines were abolished (Table 2). Instead, as shown in Table 1, there was a significant decrease in α-carotene (**5a**) concentration and a significant increase in concentration of the α-carotene derivative zeinoxanthin (**7**).

97B3 and 97BKB: over-expression of *CYP97B3* the previously uncharacterized carotenoid hydroxylase candidate (97B3 lines) resulted in modest but statistically significant shifts in the abundance of α-carotene (**5a**) and its derivatives, including significant decreases in α-carotene (**5a**) and α-cryptoxanthin (**6**) concentrations and a significant increase in zeinoxanthin (**7**) concentration (Table 1). 97BKB lines expressing the *bkt1* ketolase gene and over expressing *CYP97B3* showed changes in concentrations of α-carotene (**5a**) and its derivatives relative to wild-type similar to those observed in 97B3 lines (Table 1). However, 97BKB plants had a significantly higher *cis*-lutein (**8**) concentration compared to the WT.

Accumulation of β-carotene derivatives in the 97B3 and 97BKB lines was also affected: 97B3 plants had a significantly lower β-cryptoxanthin (**6b**) concentration than WT plants and in 97BKB *cis*-violaxanthin accumulated to significantly higher levels than in WT. Co-expression of *bkt1* in the 97BKB lines did not significantly alter the accumulation of β-carotene-derived products.

97C1 and 97CKB: over-expression of *CYP97C1* in 97C1 lines resulted in changes in abundance of both the α- and β-carotene pathway products relative to WT. In the α-carotene (**5a**) pathway, 97C1 had significantly lower α-carotene (**5a**) and significantly higher zeinoxanthin (**7**) concentrations than WT, respectively (Table 1). In the β-carotene (**5b**) pathway, 97C1 lines exhibited a significant decrease in β-cryptoxanthin (**6b**) level (Table 2).

Co-expression of the *bkt1* gene with *CYP97C1* in 97CKB lines led to decreased α-cryptoxanthin (**6a**) concentration relative to levels in both WT and 97C1 lines (Table 1) but had no other detectable effect. *bkt1* co-expression with *CYP97C1* had no significant overall effect on the β-carotene (**5b**) pathway.

97A3 and 97AKB: over-expression of the *CYP97A3* gene in 97A3 lines significantly decreased α-carotene (**5a**) levels but otherwise had no detectable effect on accumulation of α-carotene (**5a**) derivatives (Table 1). However, plants had a higher concentration of the β-carotene derivative zeaxanthin (**9**) compared to WT plants (Table 2).

Co-expression of the *bkt1* ketolase with *CYP97A3* in 97AKB lines affected the α-carotene (**5a**) pathway (Table 1) more so than the β-carotene (**5b**) pathway (Table 2). In addition to significantly lower α-carotene concentration (similar to 97A3 plants), 97AKB plants had a significantly lower α-cryptoxanthin (**6a**) concentration, accompanied by an increase in zeinoxanthin levels (**7**) (Table 1). The 97A3 and 97AKB lines both had significantly higher zeaxanthin (**9**) concentrations relative to WT plants (Table 2).

KB: Arabidopsis KB lines expressing the *bkt1* ketolase gene alone did not yield detectable ketocarotenoid products. However, α-carotene (**5a**) accumulation was considerably reduced in KB lines compared to wild type (Table 2), consistent with results from lines in which *bkt1* and *P*450 monooxygenase hydroxylase genes were co-expressed, as discussed above. In those co-expression lines, expression of *bkt1* together with hydroxylase over-expression had little effect on accumulation of β-carotene derivatives relative to over-expression of the hydroxylases alone (Table 2), but in several cases enhanced the effect on accumulation of α-carotene hydroxylation products. A summary of all results from hydroxylase over-expression lines is presented in Table 3 and Fig. 4.

3. Discussion

Carotenoids are 40-carbon isoprenoids that are integral and essential components of the photosynthetic membranes in all plants (Fig. 1). In *Arabidopsis* and other plants, carotenoid derivatives are produced from both α- and β-carotene (**5a**/**5b**), via hydroxylation of the ε- and β-rings of α-carotene, or hydroxylation of both β-rings of β-carotene (**5b**) (Cunningham and Gantt, 1998).

Table 3
Summary of changes in carotenoid product accumulation in single hydroxylase over-expression lines and hydroxylase over-expression lines co-transformed with the *bkt1* ketolase.

Hydroxylase	Single hydroxylase transformants		Double transformants (hydroxylase with *bkt1* ketolase)	
	α-Carotene (**5a**) pathway	β-Carotene (**5b**) pathway	α-Carotene (**5a**) pathway	β-Carotene (**5b**) pathway
AtB1	↓ α-Cryptoxanthin (**6a**)	↑ β-Cryptoxanthin (**6b**) ↑ Zeaxanthin (**9**) ↑ *trans*-Violaxanthin (**11**) ↑ *cis*-Violaxanthin (**11**) ↑ *trans*-Neoxanthin (**12**)	↓ α-Carotene (**5a**) ↑ Zeinoxanthin (**7**)	
CYP97A3	↓ α-Carotene (**5a**)	↑ Zeaxanthin (**9**)	↓ α-Carotene (**5a**) ↓ α-Cryptoxanthin (**5b**) ↑ Zeinoxanthin (**7**)	↑ Zeaxanthin (**9**)
CYP97B3	↓ α-Carotene (**5a**) ↓ α-Cryptoxanthin (**6a**) ↑ Zeinoxanthin (**7**)	↓ β-Cryptoxanthin (**6b**)	↓ α-Carotene (**5a**) ↓ α-Cryptoxanthin (**5b**) ↑ Zeinoxanthin (**7**) ↑ *cis*-Lutein (**8**)	↑ *cis*-Violaxanthin (**11**)
CYP97C1	↓ α-Carotene (**5a**) ↑ Zeinoxanthin (**7**)	↓ β-Cryptoxanthin (**6b**) ↑ Zeaxanthin (**9**)	↓ α-Carotene (**5a**) ↓ α-Cryptoxanthin (**6a**) ↑ Zeinoxanthin (**7**)	

Increases or decreases in abundance (↓ or ↑) relative to levels in wild-type plants are shown, using data from Tables 1 and 2.

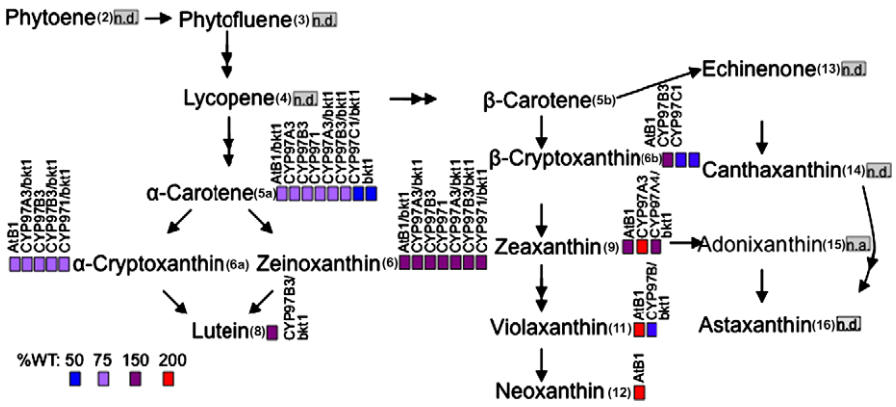

Fig. 4. Summary of effects of hydroxylase and ketolase over-expression on carotenoid levels. Levels of products and intermediates in transgenic plants overexpressing different genes and gene combinations are approximated relative to wild-type levels (50%, 75%, 150%, or 200% of wild-type level), using data from Tables 1 and 2. n.d., metabolite below detection limit; n.a., metabolite not assayed.

Previous evidence suggested that non-heme di-iron hydroxylases AtB1 and AtB2 are mostly responsible for hydroxylation activities of the β-rings in the β-carotene pathway (Sun et al., 1996; Tian and DellaPenna, 2001; Davison et al., 2002) whereas hydroxylation of the ε- and β-rings of α-carotene (**5a**) is carried out by two cytochrome *P*450 hydroxylases, CYP97A3 and CYP97C1 (Tian et al., 2004; Kim and Dellapenna, 2006). Tian et al. (2003, 2004) used double knock-out mutants of *AtB1* and *AtB2* to show that AtB1 and AtB2 have specific functions in β-carotene (**5b**) hydroxylation. However, these mutants were shown to accumulate residual β-ring hydroxylated β-carotene derivatives, suggesting presence of other hydroxylases acting on β-carotene.

While CYP97C1 is mainly responsible for ε-ring hydroxylation, there is evidence that β-ring hydroxylation deficiency in AtB1 and AtB2 can be partially compensated by up-regulation of *CYP97C1* (Tian et al., 2004). Furthermore, while *CYP97A3* encodes a β-ring hydroxylase with major activity towards the β-ring of α-carotene (**5a**), the same hydroxylase also has minor activity on the β-rings of β-carotene (**5b**) (Kim and DellaPenna, 2006). *P*450 hydroxylases thus appear to have some flexibility in their activities against carotenoid substrates, and *in vivo* activities may be dependent on the relative levels of the different carotenoid hydroxylases and on the levels of potential substrates. The conservation of not only *CYP97A3* and *CYP97C1*, but also the closely related gene *CYP97B3* in land plants within a *P*450 clan also found in green algae (Nelson, 2006) suggests that these genes play important and conserved roles in the metabolism of photosynthetic organisms.

In this study, we measured carotenoid product accumulation in *Arabidopsis* lines overexpressing carotenoid hydroxylases or expressing novel combinations of hydroxylases and the algal *bkt1* ketolase to deduce the functions and activities of carotenoid hydroxylases using an approach complementary to analysis of loss-of-function mutants, and to assess the ability to use over-expression approaches to manipulate the accumulation of carotenoid derivatives *in planta*.

When *AtB1* was overexpressed, we found significant increases of β-carotene (**5b**) pathway products (Tables 1 and 3). These results indicate greater metabolic flux into β-carotene pathways in these lines, supporting the hypothesis of Tian et al. (2003) that AtB1 and AtB2 play major roles in β-ring hydroxylation against β-carotene (**5b**). This validates the effectiveness of our approach of assessing *in vivo* functions of *Arabidopsis* carotenoid hydroxylases by over-expression in transgenic plants, shows that over-expression of these non-heme hydroxylases can have a major metabolic impact, and indicates that endogenous levels of these enzymes may be limiting for flux into β-carotene (**5b**) pathways. In the *AtB1* over-expression lines, we also detected a significant decrease in α-cryptoxanthin (**6a**). This is an indication that *AtB1*, when over-expressed, may also hydroxylate the β-ring of α-cryptoxanthin (**6a**) and thus reducing its levels, but the activity may be relatively minor and not enough to cause a detectable increase in the large lutein (**8**) pool (Fig. 4).

Over-expression of *CYP97C1* alone led to a decrease in α-carotene (**5a**) concentration but also an increase in the zeinoxanthin (**7**) concentration (Tables 1 and 3). While modest, this shift in metabolite concentrations is an indication that increased ε-ring hydroxylation by *CYP97C1* leads to increased metabolic flux away from α-carotene (**5a**) and may have caused lutein (**8**) production to shift more to the α-cryptoxanthin (**6a**) route and away from the normally major zeinoxanthin (**7**) route, leading to a decrease in zeinoxanthin (**7**) conversion to lutein (**8**) and an increase in the zeinoxanthin (**7**) pool size (Fig. 4). In addition, our data suggest that *CYP97C1* may have β-ring hydroxylase function on both α-carotene (**5a**) and β-carotene (**5b**) since there was evidence from one 97C1 line of significant increases in zeaxanthin (**9**) levels (data not shown; Table 3) and both 97C1 lines had significantly lower β-cryptoxanthin (**6b**) concentrations. This is in agreement with the finding of Tian et al. (2004) that up-regulation of *CYP97C1* leads to increased hydroxylation of β-rings of β-carotene (**5b**). The different behaviour of the two over-expression lines with respect to β-carotene (**5b**) β-ring hydroxylation may be due to differences in expression levels of the transgene in the two lines (Fig. 2D) or other uncontrolled factors.

Similarly, over-expression of *CYP97A3* also led to a modest but statistically significant decrease in α-carotene (**5a**) concentration and a doubling in the zeaxanthin (**9**) concentration, supporting the notion that CYP97A3 has activity towards the β-ring of α-carotene (**5a**) as well as some activity on the β-rings of β-carotene (**5b**) (Kim and DellaPenna, 2006). Apparently, as with *CYP97C1*, over-expression of *CYP97A3* is able to direct metabolic flux from the small pool of α-carotene (**5a**) towards its hydroxylated derivatives, and into zeaxanthin (**9**) in the β-carotene (**5b**) pathway (Table 3 and Fig. 4). These results complement the knock-out studies of Tian et al. (2003, 2004) and Kim and DellaPenna (2006) in defining the functions of these hydroxylases.

While double and triple mutant combinations involving the *AtB1*, *AtB2*, *CYP97A3* and *CYP97C1* were successful in completely blocking β-carotene (**5b**) hydroxylation, β-ring hydroxylation of α-carotene (**5a**) was still observed (Tian et al., 2004; Fiore et al., 2006; Kim and DellaPenna, 2006) and the existence of a fifth hydroxylase, acting on the β-ring of α-carotene (**5a**) but not β-carotene (**5b**) has been hypothesized (Fiore et al., 2006). The *Arabidopsis*

genome contains another CYP97 family member, *CYP97B3*, which encodes a protein 42% identical to CYP97C1 (Tian et al., 2004), and over-expression of *CYP97B3* allowed us to test the role of this enzyme in carotenoid hydroxylation. The 97B3 single over-expression lines had consistent effects on the accumulation of α-carotene in the same magnitude of the effects observed for over-expression of *CYP97A3* and *CYP97C1* (Tables 1 and 3), supporting a potential role for this hydroxylase in α-carotene (**5a**) modification. Also observed were a significant decrease in α-cryptoxanthin (**6a**) concentration and a significant increase in zeinoxanthin (**7**) concentration. One possibility is that, since over-expression seems to preferentially shift the pathway to the production of the intermediate (zeinoxanthin (**7**)) and away from the ε-ring intermediate (α-cryptoxanthin (**6a**)), 97B3 is preferentially a β-ring hydroxylase. We also found that over-expression of *CYP97B3* significantly decreased β-cryptoxanthin (**6b**) concentration (Tables 2 and 3), suggesting possible activity in β-carotene (**5b**) β-ring hydroxylation in addition to its activity against α-carotene. While these data are consistent with the preliminary finding that expression of CYP97B3 in a β-carotene (**5b**) producing *E. coli* strain leads to generation of β-cryptoxanthin (**6b**) and zeaxanthin (**9**) from β-carotene (**5b**) (Kim et al., 2005), further studies such as gene knock out and detailed biochemical characterization of CYP97B3 activity are needed to evaluate the role of CYP97B3 in carotene metabolism.

Consistent with roles in carotenoid metabolism, *in silico* analyses predict that CYP97A3 and CYP97C1 are plastid localized, based on the presence of chloroplast targeting sequences (Tian et al., 2003, 2004; Inoue, 2004), but an *in silico* analysis showed some evidence for CYP97B3 localization to mitochondria (Schuler and Werck-Reichhart, 2003). However, recent global analysis of the chloroplast proteome (Zybailov et al., 2008) provides strong empirical evidence that all three hydroxylases, CYP97A3, CYP97C1, and CYP97B3 are indeed chloroplast localized, since all are found in the chloroplast proteome. Furthermore, more recent *in silico* analyses suggest that, while there is a small probability of CYP97B3 localization to mitochondria, its mostly likely subcellular localization (like that of CYP97A3 and CYP97C1) is to chloroplasts (eFP browser, http://bar.utoronto.ca/; Winter et al., 2007). Similarly all three hydroxylases appear to have similar developmental expression patterns, with highest expression in *Arabidopsis* leaves and seedlings (eFP browser, http://bar.utoronto.ca/; Winter et al., 2007). This is consistent with overlapping and cooperative functions for all three hydroxylases in carotenoid modification. One additional approach to addressing the question of subcellular localization would be to generate CYP97B3-GPF fusions, and visualize the GPF fluorescence at the subcellular level in transgenic plants (Ro et al., 2001).

Carotenoid ketolases catalyze the addition of a keto group to the 4-position of one or both rings of the β-carotene (**5b**) to produce ketocarotenoids such as echinenone (**13**) and canthaxanthin (**14**) (Fig. 1). Ketolase genes and enzyme activity in higher plants have, to date, only been documented in *Adonis* spp. (Cunningham and Gantt, 2005; Yu et al., 2006). However, synthesis of ketocarotenoids in transgenic plants has been demonstrated in leaves and flowers of tomatoes and tobacco (Ralley et al., 2004; Gerjets et al., 2007; Zhu et al., 2007), tubers of potatoes (Gerjets and Sandmann, 2006; Morris et al., 2006), flowers of *Lotus japonicus* (Suzuki et al., 2007), seeds of *Arabidopsis* (Stålberg et al., 2003), and roots of carrot (Jayaraj et al., 2008) by expression of heterologous ketolase genes. In contrast, we found that the KB transgenic *Arabidopsis* lines expressing a *bkt* ketolase gene from *H. pluvialis*, engineered to target the bkt1 protein to the chloroplast, did not accumulate detectable levels ketocarotenoids in rosette leaves. Stålberg et al. (2003) found that the yield of ketocarotenoids in transgenic *Arabidopsis* plants they analyzed were low, even with the co-transformation of a phytoene synthase construct to boost the carotenoid content. Substrate availability and differences in temporal expression of the introduced genes in relation to endogenous biosynthesis of carotenoids are all factors that could contributing to low yields of ketocarotenoids in transgenic plants. Recent studies in tobacco (Gerjets et al., 2007; Zhu et al., 2007), indicate that it is possible to achieve accumulation of ketocarotenoids in leaves, flower petals, and flower nectaries by expression of a cyanobacterial ketolase gene. However, accumulation of the ketocarotenoid astaxanthin (**16**) was not observed in these transgenic lines. It is possible that ketocarotenoids formed in our KB and AtBKB lines, but were below the level of detection, or were among minor carotenoid peaks for which lack of standards precluded product identification.

Unexpectedly, the only difference in carotenoid content in the KB lines relative to WT and AtB1 lines was a decrease in α-carotene (**5a**) content (Table 1), suggesting that expression of the *bkt1* gene leads to increased metabolic flux away from the relatively small endogenous α-carotene (**5a**) pool. A similar decrease in β-carotene (**5b**) levels may have been expected in *bkt1* expressing lines, but no statistically significant decrease in β-carotene (**5b**) levels in these lines was observed. The much larger β-carotene (**5b**) pool size (~30X higher than α-carotene (**5a**); Tables 1 and 2) may be responsible for the lack of a significant effect of *bkt1* activity in depleting β-carotene (**5b**) content the leaves examined. Consistent with our finding that *bkt1* expression depletes α-carotene (**5a**) levels in *Arabidopsis* rosette leaves, expression of the same *bkt1* ketolase gene in *Arabidopsis* (Stålberg et al., 2003) and potato (Morris et al., 2006), resulted in detectable accumulation of 4-keto-lutein (3,3′-dihydroxy-β,ε-carotene-4-one), an α-carotene derivative, in seeds and tubers, respectively. Although we did not detect 4-keto-lutein in our transgenic lines, other β-ring derivatives of α-carotene for which we had no standards could have been produced.

Generation of large changes in carotenoid metabolic flux by transfer of a ketolase transgene may require co-transformation with a hydroxylase gene to provide sufficient levels of the appropriate hydroxylated carotenoid substrate (Ralley et al., 2004; Gerjets et al., 2007). With this in mind, we co-transformed the *bkt1* gene with each of the four carotenoid hydroxylase genes, but no ketocarotenoids were detected in any representative of the co-transformed lines, AtBKB, 97AKB, 97BKB, and 97CKB. However, in all co-transformants, unexpected differences in product accumulation relative to transformants expressing the hydroxylases alone were observed, suggesting that hydroxylation activity, particularly in the α-carotene (**5a**) pathway, was altered in the double transformants. This effect was most obvious in the AtBKB lines, where increases in multiple β-carotene hydroxylated derivatives resulting from over-expression of AtB1 were abolished by co-expression of the ketolase. A decrease of the α-carotene (**5a**) level was associated with an increase of zeinoxanthin (**7**) (β-ring hydroxylated α-carotene). Thus, our data suggest that co-expression *AtB1* and *bkt1* decreases β-ring hydroxylation of β-carotene (**5b**), and increases β-ring hydroxylation of α-carotene (**5a**).

Comparison of the AtB1 and bkt proteins shows that both enzymes belong to membrane-intergral, di-iron oxygenase enzymes which share common amino acid residues such as histidine motifs and a transmembrane helix (Cunningham and Gantt, 1998). The *bkt1* ketolase has been suggested to be mechanistically related to AtB1 since both enzymes require the presence of conserved histidine residues for activity (Bouvier et al., 1998; Ye et al., 2006). Another example of similarity between ketolase and hydroxylase proteins is evident in the *Adonis* ketolase polypeptide, which has more than 60% similarity to *Arabidopsis* AtB1 β-carotene hydroxylases (Cunningham and Gantt, 1998; Shanklin and Cahoon, 1998; Cunningham and Gantt, 2005). Sun et al. (1996) speculated that the AtB1 normally associates with a second β-hydroxylase (or with an ε-hydroxylase) to form a heterodimer and that an N-terminal

region of AtB1 N mediates these subunit interactions. Thus, uncharacterized interactions of the AtB1 hydroxylase with other membrane localize partners, possibly including *bkt1*, could alter the enzymatic properties of the hydroxylase, shifting the substrate preference of AtB1 from β-carotene (**5b**) and its derivatives to α-carotene (**5a**) in the presence of *bkt1*. Further investigation along this line would be worthwhile.

While our interpretation of enzyme functions based on product accumulation in overexpressing lines does not account for interconversion between α-carotene (**5a**) and β-carotene (**5b**) products *in vivo*, our results are consistent with autonomous and separate pathways.

4. Concluding remarks

In conclusion, our study focussed on the over-expression of hydroxylases and the *bkt1* ketolase in *Arabidopsis* has confirmed the roles that the three carotenoid hydroxylases, AtB1, CYP97A3, and CYP97C1, play in the carotenoid pathways and shows that mis-expressing of the individual hydroxylases can impact carotenoids metabolic flux, with the effect of *AtB1* over-expression on β-carotene metabolism being the most pronounced. In addition we provide new evidence for potential for dual activities of carotenoid hydroxylases, working in both the α- and β-carotene pathways and evidence for a possible function of CYP97B3 in carotenoid metabolism, as a possible β-ring hydroxylase. This work shows that it is possible to alter flux through carotenoid metabolic pathways, and alter intermediate accumulation, by over-expression of hydroxylases with or without co-expression of a heterologous ketolase. However, many metabolic changes were relatively modest, and unexpected changes in pathway flux were demonstrated in different transgenic lines, suggesting that further information on the enzymatic regulation of flux through carotene modification pathways is required to facilitate rational metabolic engineering of the pathways.

Table 4
Gene-specific primers to amplify the coding regions of β-carotene hydroxylase (AtB1) and CYP97 family (CYP97A3, CYP97B3, CYP97C1) from cDNA of *Arabidopsis* ecotype Col-0.

Primer	Gene	Primer sequences
AtB1 F[a]	AtB1	5′-CACCATGGCGGCAGGA CTCTCAAC-3′
AtB1 R[b]	AtB1	5′-TCAAGAACTCGAACTCGACCC-3′
97A3 F	CYP97A3	5′-CACCCATGGCTATGGCCTTTCCTCTT-3′
97A3 R	CYP97A3	5′-TTAAGAAAGAGCAGATGAAAC-3′
97B3 F	CYP97B3	5′-CACCATGGTAGCAGCCATGGCTTT-3′
97B3 R	CYP97B3	5′-TCACTTTGATCTTCTCTTTAG-3′
97C1 F	CYP97C1	5′-CACCATGGAGTCTTCACTCTTTTCT-3′
97C1 R	CYP97C1	5′-TTACCTTTGGCTCACCTTCAT-3′

[a] F: forward.
[b] R: reverse.

5. Experimental

5.1. Binary vector construction

Hydroxylases: coding regions of β-carotene hydroxylase (AtB1, At4g25700) and CYP97 family proteins (CYP97A3, At1g31800; CYP97B3, At4g15110; CYP97C1, At3g53130) were isolated from cDNA of the *Arabidopsis* ecotype Col-0 (*A. thaliana*). Coding regions for AtB1, CYP97A3, CYP97B3 and CYP97C1 were amplified by PCR using the PWO DNA polymerase (Roche Applied Science, Indianapolis, IN). To obtain the full length cDNAs of genes by PCR, gene-specific primers were used (see Table 4).

The genes were placed under the control of the double CaMV35S promoter in the pSM-3 vector containing a hygromycin resistance (hyg^R) gene as a plant selectable marker by PCR amplification of cDNAs using gene-specific primers containing restriction enzyme recognition sites. Gene-specific primers with *XbaI*, *KpnI*, *XmaI* or *BamHI* restriction enzyme sites (underlined) were used for PCR (Table 5). The PCR products were digested with each enzyme and ligated into the corresponding site of pSM-3. These fusion constructs were named as pAtB1 (double CaMV35S-AtB1), p97A3 (double CaMV35S-97A3), p97B3 (double CaMV35S-97B3) and p97C1 (double CaMV35S-97C1), respectively.

Ketolase: the double CaMV35S-ketolase construct (pKB) harboring the *H. pluvialis bkt1* ketolase gene (CrtO, Keto-2a (Jayaraj et al., 2008), chloroplast targeting, transit peptide) and *bar* selectable marker genes, was used for this study. To facilitate selection of *Arabidopsis* co-transformants with each *P*450 hydroxylase transgene, the hygromycin resistance gene (hyg^R) was eliminated by *Xho*I digestion and re-ligation. PCR with gene-specific primers (forward: 5′-ATGAAAAAGCCTGAACTCACCGCG-3′ and reverse: 5′-TCTACACA GCCATCGGTCCAG AC-3′) confirmed excision of the gene. *Agrobacterium tumefaciens* strain GV3101 was transformed with each of the fusion constructs (pAtB1, p97A3, p97B3, p97C1 and pKB) by heat shock. Transformants were selected on Luria–Bertani media containing rifampicin (25 mg l^{-1}), gentamycin (25 mg l^{-1}) and kanamycin (50 mg l^{-1}), and the presence of the fusion constructs were verified by PCR.

5.2. Plant transformation and selection

A. tumefaciens strain GV3101 carrying the fusion constructs was grown at 28–30 °C and transformed into *A. thaliana* (Col-0), using the floral dip method (Clough and Bent, 1998) with 0.05% (v/v) Silwet L-77 (Lehle Seeds, Round Rock, TX) and 5% sucrose. *Agrobacterium* strains with AtB1 and *P*450 hydroxylase constructs were

Table 5
Gene-specific primers containing the restriction enzyme recognition sites to amplify the each gene coding region for the fusion binary vector constructs.

Primer	Construct	Primer sequence
AtB1 (XbaI) F[a]	pAtB1	5′-CAGGCT**TCTAGA**ATCATGGCGGCAGGACTCT-3′[c]
AtB1 (KpnI) R[b]	pAtB1	5′-GAGCCA**GGTACC**TCAAGAACTCGAACTCGACC-3′
97A3 (XmaI) F	p97A3	5′-TCCGTCCT**CCCGGG**TATGGCTATGGCCTTTCCT-3′
97A3 (XmaI) R	p97A3	5′-ACGTAGGGT**CCCGGG**TTAAGAAAGAGCAG ATG-3′
97B3 (BamHI) F	p97B3	5′-TGCCCCA**GGATCC**GCAATGGTAGCAGCCATGG-3′
97B3 (KpnI) R	p97B3	5′-GCCCGTC**GGTACC**TCACTTTGATCTTCTCTTTAGTT-3′
97C1 (XbaI) F	p97C1	5′-CACGTCCGC**TCTAGA**ATGGAGTCTTCACTCTTT-3′
97C1(BamHI) R	p97C1	5′-GTGTACC**GGATCC**TTACCTTTGGCTCACCTTC-3′

[a] F: forward.
[b] R: reverse.
[c] Enzyme recognition site underlined and in bold.

named GV3101/pAtB1, GV3101/p97A3, GV3101/p97B3, and GV3101/p97C1, respectively, and the *Agrobacterium* strain with the ketolase (*bkt1*) construct was named GV3101/pKB.

For co-transformation, GV3101/pKB was mixed with an equal volume of the appropriate GV3101/hydroxylase strain. Dipped plants were covered with black plastic wrap (for 24 h) to maintain high humidity and were kept in the potting room for drying after seed set. Seeds were harvested and sterilized with EtOH–H_2O (7:3 and 95:5, v/v). Single transformed plants were designated as AtB1, 97A3, 97B3, 97C1 and KB, respectively. The seedlings (T1) of primary hydroxylase transformed plants (T_0) were selected on Murashige–Skoog (MS) media containing hygromycin (50 mg l^{-1}; Invitrogen, Ontario, Canada). KB seedlings (T1) were selected either on MS media with either glufosinate-ammonium (50 mg l^{-1}; Sigma–Aldrich, Canada) or by spraying with 0.1% (v/v) BASTA (glufosinate Final EV150, AgrEvo EH, Paris, France). For selection of co-transformed plants (designated as AtBKB, 97AKB, 97BKB and 97CKB), seedlings (T1) of primary co-transformed plants (T_0) were first selected on MS media containing hygromycin (50 mg ml^{-1}), transferred to soil mix (Sunshine Mix 5; SunGro, Seba Beach, Alberta, Canada) and grown to maturity. T1 co-transformed lines harboring both ketolase and hydroxylase T-DNA insertions were identified by PCR analysis of genomic DNA to ensure that both ketolase and hydroxylase genes were present in these plants. Seeds of T1 plants were harvested and selected on MS media supplemented with hygromycin. Surviving seedlings (T2) were transferred to soil and T2 co-transformant lines identified by spraying with BASTA every 7 days after potting. Plants were grown under a 12 h photoperiod (100–120 μmol m^{-2} s^{-1}; 22 °C light period, 18 °C dark period). To identify homozygous lines, the segregation pattern of hygromycin and BASTA resistances of T2 lines was determined by growing T3 seedlings on MS media (MS, MS with 50 mg l^{-1} hygromycin, and/or MS with 50 mg l^{-1} BASTA). T3 homozygous plants were grown on MS media without selection and leaves were harvested for HPLC analysis.

5.3. Genomic DNA

Plant genomic DNA was extracted from 4 week old leaves (0.1 g) of wild type *Arabidopsis* Col-0 plants and transgenic T1 lines with the Nucleon PhytoPure Kit (Amersham Biosciences, Quebec, Canada). To confirm transgene presence, a primer located in the double CaMV35S promoter was used in combination with gene-specific primers in a PCR (Table 6). PCR conditions were 94 °C for 2 min, 94 °C for 45 s, 57 °C for 30 s, 72 °C for 45 s (30 cycles), 72 °C for 7 min and 10 °C for 5 min.

5.4. RNA isolation

Four to five week old leaves from each T2 line were used for transcript analysis and to select representative lines with high transcript levels. Total RNA was extracted from leaf samples (0.1 g) using the RNeasy Plant Mini Kit (QIAgen, Valencia, CA) and was treated with RNase-free DNase (QIAgen, Valencia, CA). Total RNA was quantified in a UV–visible spectrophotometer (Biospec-1601, Shimadzu, Columbia, MD) and the quality evaluated on an agarose gel (1%, v/w).

Table 6
Primers for PCR confirmation of transgene presence in transformed *Arabidopsis* lines.

Primer name	Orientation	Primer sequence
2X 35S[a]	F[b]	5′-TGACGCACAATCCCACTATCCTTCGCAAGACCCT-3′
AtB1_R2	R[c]	5′-TCTCACCTCCCTCCATTTGCCAA-3′
97A3_R2	R	5′-CAATGCAGGAACAATGGCACGCC-3′
97B3_R2	R	5′-TCCCATAATCGGCTCTAAGATCTCA-3′
97C1_R2	R	5′-CAATCACAGACAAATACCTCCTG-3′

[a] Double CaMV 35S promoter.
[b] F: forward.
[c] R: reverse.

5.5. cDNA synthesis and RT-PCR analysis

The first-strand cDNA synthesis was performed using 2 μg of total RNA/20 μl reaction with the Superscript II Reverse Transcriptase (Invitrogen, Carlsbad, CA). Actin was used to normalize for variation in cDNA concentrations. Actin specific primers are described in Table 7. The PCR condition was: 94 °C for 3 min, 94 °C for 30 s, 63 °C for 30 s, and 72 °C for 1 min, followed by a final extension at 72 °C for 3 min (30 cycles). After normalizing the amount of cDNA of each gene with actin, the transcript level of each sample was compared. The gene-specific PCR primers were used to amplify a cDNA fragment of AtB1 (Table 7). The PCR conditions were: 94 °C for 2 min, 94 °C for 45 s, 56–58 °C for 30 s, and 72 °C for 40 s, followed by a final extension at 72 °C for 3 min (30 cycles). PCR products were separated by electrophoresis on a 1% agarose gel and visualized under ultraviolet light after staining with ethidium bromide. The PCR band intensities were measured using Alpha Imager software.

5.6. Pigment extraction and HPLC analysis

Approximately 50–150 mg of leaf tissue was extracted with MeOH–MeOH (5 ml, 1:1). The samples were saponified by 1 ml of 40% methanolic KOH using 10% pyrogallol (400 μl) as an antioxidant. Samples were incubated at 60 °C for 30 min under nitrogen atmosphere. H_2O (3 ml) was added to each tube and the samples were extracted twice with hexane (4 ml) and brought to 10 ml with hexane. Three methods were used for analysis and quantitative analysis of carotenoids in the samples.

(1) To determine which carotenoids were detectable in the hexane extracts, these were dried under vacuum in a SpeedVac™. The extracts were redissolved in EtOAc and diluted in CH_3CN–iPrOH (9:1, v/v). The HPLC system consisted of a computer data system, an autosampler maintaining samples at 20 °C, a column heater at 31 °C, a programmable ultraviolet visible detector and a fluorescence detector (Thermo Separation Products, Fremont, CA). The separation was performed isocratically on a Spherisorb ODS2 column (3 μm, 4.0 × 250 mm with titanium frits, ES Industries, West Berlin, NJ) protected by a Javelin™ guard column containing a similar stationary phase (Thermo Electron Corp., Bellefonte, PA). The mobile phase consisted of CH_3CN/dioxane/iPrOH (100 mM ammonium acetate)/Et_3N (80/15/5/0.1) at a flow rate of 1.0 ml min^{-1}.

Table 7
Primers for RT-PCR measurement of transgene expression.

Primer name	Orientation	Primer sequence
AtB1_RT	F[a]	5′-GAGAACGATGAGAGACCGGA-3′
AtB1_RT	R[b]	5′-TCGAACTCGACCCGGAGCCCGA-3′
97A3_RT	F	5′-CGTACTCTCGGAGATCGAAC-3′
97A3_RT	R	5′-TATCAAGTGTCAAACGAGAG-3′
97B3_RT	F	5′-GTTGTCATCTCAGATCCCATTAT-3′
97B3_RT	R	5′-GCCGGTCATCAATGTCAACAC-3′
97C1_RT	F	5′-TGGAGTCTTCACTCTTTTCTCC-3′
97C1_RT	R	5′-TACCTTTGGCTCACCTTCATATAC-3′
Actin	F	5′-GCGACAATGGAACTGGAAT-3′
Actin	R	5′-GGATAGCATGTGGAAGTGCATACC-3′
Keto	F	5′-GCAATG GTGGAAGAGTAAAGTGC-3′
Keto	R	5′-GTTGTGGTGCTCCCAATGCTTGCGG-3′

[a] F: forward.
[b] R: reverse.

The diode array detector with light pipe flow cell was programmed to monitor carotenoids at 450 nm and scanned from 280 to 520 nm.

(2) For quantification of individual carotenoids (shown in Tables 1 and 2), hexane extracts were injected onto a Chromegabond Diol normal-phase column (3 μm, 4.0 × 150 mm, ES Industries, West Berlin, NJ) protected by an Amino SecurityGuard™ guard column (Phenomenex, Torrence, CA) and eluted isocratically with hexane–iPrOH (96:4, v/v) at a flow rate of 1.5 ml min^{-1}. Carotenoids were monitored at 450 nm using a programmable wavelength detector. Astaxanthin was analyzed by normal-phase HPLC in non-saponified samples. Analytes are quantified using external authentic standards to calculate response factors.

(3) For confirmation of peak identities and to exclude the possibility of overlapping peaks, concentrated samples from individual peals were further separated by C30 gradient HPLC with diode array detection on an analytical YMC C30 column (3 μm, 4.6 × 250 mm, Waters, Milford, MA) with phase A THF/H_2O (4:1, v/v with 20 mM ammonium acetate and 0.05% Et_3N), phase B CH_3CN/0.05% Et_3N, phase C EtOAc/0.05% Et_3N. The following program was used with a flow rate of 1.0 ml min^{-1}: 15% A throughout, 75% B and 10% C 2 min, to 50% B and 35% C for 23 min, to 17% B and 70% C for 7 min, 10% B and 75% C for 18 min, hold for 2 min then return to initial conditions 8 min, equilibration for 10 min before the next injection. Carotenoids were monitored at 450 nm and scanned from 280 to 500 nm and quantified using standard curves of authentic standards. All methods were adapted from Craft and Furr (2004).

5.7. Statistical analysis

Because of the non-orthogonality (unequal cell sizes) of the HPLC data, they were analyzed by Least-Squares Analysis of Variance (Spector, 1980) using the JMP statistics software (JMP-IN version 5.1.2, SAS Institute, Cary, NC) with the following statistical model:

$$Y_{ijk} = \mu + C_i + L(C)_{ij} + E_{ijk}$$

Y is one of the carotenoid products detected, C denotes all the treatments to be compared (WT, AtB1, AtBKB, 97A3, 97AKB, 97B3, 97BKB, 97C1, 97CKB, and KB), and $L(C)$ denotes two lines nested in each treatment. E denotes the error term for the model. Mean separation of significant factors determined by the Least-Square Analysis was done by Student's t-tests. Except for 97CKB and WT, which was represented by a single line with two independent leaf samples, values given in the tables are means of four measurements: two lines, with two independent leaf samples per line. Each sample value is the mean of two injections.

Acknowledgements

We thank Dr. Dean Dellapenna (Michigan State University, US) for providing helpful suggestions in development of the manuscript, Dr. Raju Datla (National Research Council Canada) for providing the double CaMV35S promoter and Dr. Robert Devlin (Fisheries and Oceans Canada) for ketolase *bkt1* cDNAs. This research was supported by a Strategic Grant from the Natural Sciences and Engineering Research Council of Canada to CJD and KMC and by a University of British Columbia Graduate Fellowship to J-EK.

References

Blasco, F., Kauffmann, I., Schmid, R.D., 2004. CYP175A1 from *Thermus thermophilus* HB27, the first β-carotene hydroxylase of the *P*450 superfamily. Appl. Microbiol. Biotechnol. 64, 671–674.

Bouvier, F., Backhaus, R.A., Camara, B., 1998. Induction and control of chromoplast-specific carotenoid genes by oxidative stress. J. Biol. Chem. 273, 30651–30659.

Britton, G., 1998. Overview of carotenoid biosynthesis. In: Britton, G., Liaaen-Jensen, Pfander H. (Eds.), Carotenoids Biosynthesis and Metabolism, vol. 3. Birkhauser Verlag, Basel, pp. 13–147.

Clough, S.J., Bent, A.F., 1998. Floral dip: a simplified method for Agrobacterium-mediated transformation of *Arabidopsis thaliana*. Plant J. 16, 735–743.

Craft, N.E., Furr, H.C., 2004. Improved HPLC analysis of retinol and retinyl esters, tocopherols, and carotenoids in human serum samples for the NHANES. FASEB J. 18, A534.

Cunningham, F.X., Gantt, E., 1998. Genes and enzymes of carotenoid biosynthesis in plants. Annu. Rev. Plant. Physiol. Plant. Mol. Biol. 49, 557–583.

Cunningham, F.X., Gantt, E., 2005. A study in scarlet: enzymes of ketocarotenoid biosynthesis in the flowers of *Adonis aestivalis*. Plant J. 41, 478–492.

Davison, P.A., Hunter, C.N., Horton, P., 2002. Overexpression of β-carotene hydroxylase enhances stress tolerance in *Arabidopsis*. Nature 418, 203–206.

DellaPenna, D., 2004. Carotenoid synthesis and function in plants: insights from mutant studies in *Arabidopsis thaliana*. In: Frank, H.A., et al. (Eds.), The Photochemistry of Carotenoids, vol. 8. Kluwer Academic, Dordrecht, pp. 21–37.

Fiore, A., Dall'Osto, L., Fraser, F.D., Bassi, R., Giuliano, G., 2006. Elucidation of the β-carotene hydroxylation pathway in *Arabidopsis thaliana*. FEBS Lett. 580, 4718–4722.

Galpaz, N., Ronen, G., Khalfa, Z., Zamir, D., Hirschberg, J., 2006. A chromoplast-specific carotenoid biosynthesis pathway is revealed by cloning of the tomato white-flower locus. Plant Cell 18, 1947–1960.

Gerjets, T., Sandmann, G., 2006. Ketocarotenoid formation in transgenic potato. J. Exp. Bot. 57, 3639–3645.

Gerjets, T., Sandmann, M., Zhu, C., Sandmann, G., 2007. Metabolic engineering of ketocarotenoid biosynthesis in leaves and flowers of tobacco species. Biotechnol. J. 2, 1263–1269.

Huang, J.G., Chen, F., Sandmann, G., 2005. Stress-related differential expression of multiple β-carotene ketolase genes in the unicellular green alga *Haematococcus pluvialis*. J. Biotechnol. 122, 176–185.

Hundle, B.S., Alberti, M., Nievelstein, V., Beyer, P., Kleinig, H., Armstrong, G.A., Burke, G.A., Kleing, H., Hearst, J.E., 1994. Functional assignment of *Erwinia herbicola* Eho10 carotenoid genes expressed in *Escherichia coli*. Mol. Gen. Genet. 245, 406–416.

Inoue, K., 2004. Carotenoid hydroxylation – *P*450 finally! Trends Plant Sci. 9, 515–517.

Jayaraj, J., Devlin, R.H., Punja, Z.K., 2008. Metabolic engineering of novel ketocarotenoid production in carrot plants. Trans. Res. 17, 489–501.

Kim, J., DellaPenna, D., 2006. Defining the primary route for lutein synthesis in plants: the role of *Arabidopsis* carotenoid β-ring hydroxylase CYP97A3. Proc. Natl. Acad. Sci. USA 103, 3474–3479.

Kim, J.E., Punja, Z.K., Douglas, C.J., 2005. Co-expression of *Arabidopsis thaliana* cytochrome *P*450 enzymes and NADPH-cytochrome *P*450 reductase in *Escherichia coli*: testing the function of candidate β-carotene hydroxylases. In: *P*450 Systems and Regulation, Proceedings of 14th International Conference on Cytochromes *P*450, Dallas, TX, 2005. Medimond S.r.l, Italy, pp. 115–120.

Linden, H., 1999. Carotenoid hydroxylase from *Haematococcus pluvialis*: cDNA sequence, regulation and functional complementation. Biochim. Biophys. Acta 1446, 203–212.

Martín, J.F., Gudiña, N.E., Barredo, J.L., 2008. Conversion of β-carotene into astaxanthin: two separate enzymes or a bifunctional hydroxylase-ketolase protein? Microb. Cell. Fact. 7, 3 doi:10.1186/1475-2859-7-3.

Masamoto, K., Misawa, N., Kaneko, T., Kikuno, R., Toh, H., 1998. β-Carotene hydroxylase gene from the cyanobacterium *Synechocystis* sp. PCC6803. Plant. Cell Physiol. 39, 560–564.

Misawa, N., Nakagawa, M., Kobayashi, K., Yamano, S., Izawa, Y., Nakamura, K., Harashima, K., 1990. Elucidation of the *Erwinia uredovora* carotenoid biosynthetic pathway by functional analysis of gene products expressed in *Escherichia coli*. J. Bacteriol. 172, 6704–6712.

Misawa, N., Satomi, Y., Kondo, K., Yokoyama, A., Kajiwara, S., Saito, T., Ohtani, T., Miki, W., 1995. Structure and functional analysis of a marine bacterial carotenoid biosynthesis gene cluster and astaxanthin biosynthetic pathway proposed at the gene level. J. Bacteriol. 177, 6575–6584.

Morris, W.L., Ducreux, L.J.M., Fraser, P.D., Millam, S., Taylor, M.A., 2006. Engineering ketocarotenoid biosynthesis in potato tubers. Metab. Eng. 8, 253–263.

Nelson, D.R., 2006. Plant cytochrome *P*450s from moss to poplar. Phytochem. Rev. 5, 193–204.

Niyogi, K.K., 1999. Photoprotection revisitd: genetic and molecular approaches. Annu. Rev. Plant. Physiol. Plant. Mol. Biol. 50, 333–359.

Quinlan, R.F., Jaradat, T.T., Wurtzel, E.T., 2007. *Escherichia coli* as a platform for functional expression of plant *P*450 carotene hydroxylases. Arch. Biochem. Biophys. 458, 146–157.

Ralley, L., Enfissi, E.M.A., Misawa, N., Schuch, W., Bramley, P.M., Fraser, P.D., 2004. Metabolic engineering of ketocarotenoid formation in higher plants. Plant J. 39, 477–486.

Renstrom, B., Berger, H., Liaaen-Jensen, S., 1981. Esterified, optical pure (3S,3′S)-astaxanthin from flowers of *Adonis annua*. Biochem. System. Ecol. 9, 249–250.

Ro, D.K., Mah, N., Ellis, B.E., Douglas, C.J., 2001. Functional characterization and subcellular localization of poplar (*Populus trichocarpa* × *Populus deltoides*) cinnamate 4-hydroxylase. Plant Physiol. 126, 317–329.

Schuler, M.A., Werck-Reichhart, D., 2003. Functional genomics of *P*450s. Annu. Rev. Plant. Biol. 54, 629–667.

Shanklin, J., Cahoon, E.B., 1998. Desaturation and related modifications of fatty acids. Ann. Rev. Plant. Physiol. Plant. Mol. Biol. 49, 611–641.

Spector, P.E., 1980. Handling non-orthogonal analysis of variance: a review of techniques. Eval. Rev. 4, 843–855.

Stålberg, K., Lindgren, O., Ek, B., Höglund, A.-S., 2003. Synthesis of ketocarotenoids in the seed of *Arabidopsis thaliana*. Plant J. 36, 771–779.

Sun, Z., Gantt, E., Cunningham, F.X., 1996. Cloning and functional analysis of the β-carotene hydroxylase of *Arabidopsis thaliana*. J. Biol. Chem. 271, 24349–24352.

Suzuki, S., Nishihara, M., Nakatsuka, T., Misawa, N., Ogiwara, I., Yamamura, S., 2007. Flower color alteration in *Lotus japonicus* by modification of the carotenoid biosynthetic pathway. Plant Cell Rep. 26, 951–959.

Tian, L., DellaPenna, D., 2001. Characterization of a second carotenoid β-hydroxylase gene from *Arabidopsis* and its relationship to the LUT1 locus. Plant. Mol. Biol. 47, 379–388.

Tian, L., DellaPenna, D., 2004. Progress in understanding the origin and functions of carotenoid hydroxylases in plants. Arch. Biochem. Biophys. 430, 22–29.

Tian, L., Magallanes-Lundback, M., Musetti, V., DellaPenna, D., 2003. Functional analysis of β- and ε-ring caortneoid hydroxylase in *Arabidopsis*. Plant Cell 15, 1320–1332.

Tian, L., Musetti, V., Kim, J., Magallanes-Lundback, M., DellaPenna, D., 2004. The *Arabidopsis LUT1* locus encodes a member of the cytochrome *P*450 family that is required for carotenoid ε-ring hydroxylation activity. Proc. Natl. Acad. Sci. USA 101, 402–407.

Winter, D., Vinegar, B., Nahal, H., Ammar, R., Wilson, G.V., Provart, N.J., 2007. An "electronic fluorescent pictograph" browser for exploring and analyzing large-scale biological data sets. PLoS ONE 2, e718.

Ye, R.W., Stead, K.J., Yao, H., Heo, H., 2006. Mutational and functional analysis of the β-carotene ketolase involved in the production of canthaxanthin and astaxanthin. Appl. Environ. Microbiol. 72, 5829–5837.

Yu, B., Lydiate, D.J., Schäfer, U.A., Hannoufa, A., 2006. Characterization of a β-carotene hydroxylase of *Adonis aestivalis* and its expression in *Arabidopsis thaliana*. Planta 226, 181–192.

Zhu, C., Gerjets, T., Sandmann, G., 2007. *Nicotiana glauca* engineered for the production of ketocarotenoids in flowers and leaves by expressing the cyanobacterial *crtO* ketolase gene. Trans. Res. 16, 813–821.

Zybailov, B., Rutschow, H., Friso, G., Rudella, A., Emanuelsson, O., Sun, Q., van Wijk, K.J., 2008. Sorting signals, N-terminal modifications and abundance of the chloroplast proteome. PLoS ONE 3, e1994.